Atomic Spectra

Object

To become familiar with the construction and operation of a high quality grating spectrograph.

To observe the Balmer series of atomic hydrogen and deuterium, and to determine the finite mass Rydberg constant of the series formulae.

To observe and interpret spin-orbit doublets and triplets in alkali spectra.

References

1. Serway, Moses and Moyer: Modern Physics, pp. 88-93 (Rutherford nuclear model), 93-106 (atomic structure and electron spectra)

2. D. W. Preston and E. R. Dietz: The Art of Experimental Physics, pp. 397-399, resolution of optical instruments

3. Beiser: Concepts of Modern Physics, pp. 131-161 (atomic structure and electron spectra)

4. Eisberg and Resnick: Quantum Physics of Atoms, Molecules, Solids, Nuclei and Particles, pp. 95-119, p286 (relativistic correction)

5. Sawyer: "Experimental Spectroscopy Chapter 4, for general theory of spectrographs: Sec. 88, 89 and 90 for method of measuring the wavelengths of spectrum lines.

6. Zaidel et. al.: "Tables of Spectral Lines" (Plenum, New York, 1970) for wavelengths of lines in the spectrum of mercury.

7. Kodak Plates and Films for Science and Industry, for techniques for developing films and plates and for choice of photographic material.

8. E. Hecht: Optics, 2nd. Ed, 1987, Addison-Wesley. Chapter 5, pages 163-169 (prisms)

9. G. R. Fowles: Introduction to Modern Optics, 2nd Ed., Holt, Rhinehart, Winston, 1975. Pages 226-232 (hydrogen spectra); pp. 243-248 (selection rules, probability densities, transition rates)

10. Jerkins and White: Fundamentals of Optics (instrumentation)

11. Monk: Light: Principles and Experiment, 1937 (instrumentation)

12. A.C. Melissinos: Experiments in Modern Physics, Chapter 28-43 (hydrogen spectrum, constant-deviation prism spectrometer

1**3.** L. I Schiff, Quantum Mechanics, McGraw-Hill, Chapter IV (hydrogen wave function)

14. A. Ruark and H. Urey, Atoms, Molecules and Quanta, p562 (hydrogen wave function), p 128-131 (Sommerfeld's elliptic orbits), p132-6 (relativistic corrections), p699 (multiplet intensity ratios)

15. Handbook of Chemistry and Physics, 75th Ed. (Index of refraction vs. wavelength for air)

16. H. E. White, Introduction to Atomic Spectra, McGraw-Hill (1934)

17. W. E. Lamb, Jr. and R. C. Retherford: The Structure of the Hydrogen Atom by a Microwave Method, Phys. Rev. 72, 241 (1957)

18. S. Bjorken and S. Drell: Relativistic Quantum Mechanics, McGraw-Hill (1964)

19. A. S. Coolidge: Experimental Verification of the Theory of the Continuous Spectra of H^2 and D^2, Phys. Rev. 65, 236 (1944?)

20. I.I. Sobelman: Atomic Spectra and Radiative Transitions, 2nd ed., Springer-Verlag (1992): QC454.A8S62, ISBN 0-387-54518-2; (absorption cross section, p205)

21. H. Haken & H.C. Wolf: Atomic and Quantum Physics, 2nd. ed., Springer-Verlag (1987), QC173.H17513, ISBN 0-387-17702-7

22. T.F. Gallagher: Rydberg Atoms, Cambridge (1994), QC454.A8S27, ISBN 0-521-38531-8

23. A. Pais: George Uhlenbeck and the Discovery of Electron Spin, Physics Today v42, #12, December 1989, p34-40

24. G. Herzberg, Atomic Spectra and Atomic Structure, 2nd. ed., 1944 (Dover); thermal and electron discharge excitation probabilities, intensity ratios, pp. 159 - 162

25. J. F. James: A Student's Guide to Fourier Transforms, with applications in physics and engineering, Cambridge 1995, QC 20.7.F67.J36, ISBN 0 521 46298 3 (hardback), 0 521 46829 9 (paperback); diffraction grating, p 48; apodising mask p51; line shapes, p83-87.

26. 1995 Annual Reference Catalog for Optics, Science and education, Edmund Scientific Corp., Edmund Scientific Corporation, Order Dept., Edscorp Bldg., Barrington NJ 08007-1380

I. Theory

1. Spectrum of hydrogen

The hydrogen atom was the great workshop of non -relativistic and relativistic quantum mechanical theory in the early 20th century, due to the well-known (Coulomb) interaction, simple two-body structure and abundant experimental data. (Treatment of complex atoms (two or more electrons) introduced a new and fundamental consideration: the quantum statistics of identical fermions.) In the middle of the century, the postulation and discovery of the Lamb shift served as a crucial test of a field-theoretical picture (quantum electrodynamics) in which electrons continuously emit and reabsorb "virtual" photons and e^+-e^- pairs, with successful subtraction ("renormalization") of infinite energies to yield a small, finite net shift.

In the most elementary picture the single electron of the hydrogen atom can exist only in certain quantized bound energy states, indicated by the quantum number n = 1,2,3, etc. It was N. Bohr's (his son Aage Bohr, was also a Nobel prize winner) great contribution to provide the first simple bound state recipe involving circular orbits, soon extended to elliptical orbits by Sommerfeld and then elaborated by wave mechanics, for the quantized orbits and energies. It was shown that quantization of the orbit angular momentum in integer units of $h/2\pi$ yielded the Bohr circular orbits and the Sommerfeld elliptical orbits.

Sommerfeld observed that as in planetary Keplerian orbits (1/r potential), the total energy depends only on the length of the semi-major axis (principal quantum number n), and that a limited number of elliptical orbits (including the Bohr circular orbit) can have the same total energy while differing in the quantized integer angular momentum number l (l ranges from 0 to n-1, for each n) .

Larger n means a higher energy (less negative total energy of bound state), and an increase in the average distance between the electron and nucleus (a proton, deuteron or (unstable) triton, for hydrogen). Energy is emitted in the form of radiation of definite wavelength when an electron in a higher energy state "drops" down to a lower state. In our hydrogen experiment we will be concerned mainly with transitions which all end on the second level (n = 2, split by relativistic and intrinsic spin effects, as we will see later, as are also the "upper" states of the transition pair), for these constitute the only atomic hydrogen radiation transmitted easily through the discharge source tube and reflected strongly by the grating. Total energy (+ kinetic and - potential, net - for an electron bound to the nucleus) in hydrogen is given by

Eq. 1 $$E_n = - R_H \, hc/n^2$$

where the Rydberg constant $R_H = 2\pi^2 e^4 \mu/(h^3 c)$

and where μ (reduced mass) = $m*m_{nucleus}/(m+m_{nucleus})$ and m is the electron mass. The allowed radii are

Eq. 2 $$r_n = \frac{n^2\hbar^2}{(kme^2)} = n^2 a_0$$

where k is the electrostatic force constant.

Transitions which involve different (higher energy) initial states and the same final state are referred to as a series. The photon frequencies for a series will be given by the energy conservation relation

Eq. 3 $h\nu = E_i - E_f = +R_H\, hc \left(\frac{1}{n_f^2} - \frac{1}{n_i^2} \right)$ whence (since $\nu/c = 1/\lambda$)

Eq. 4 $$\frac{1}{l_{if}} = R_H \left(\frac{1}{n_f^2} - \frac{1}{n_i^2} \right).$$

The Rydberg constant has units of inverse length, e.g. cm^{-1} . With a proton as nucleus R_H = 109677.76 cm-1 and, for a deuteron nucleus, R_D = 109707.39 cm^{-1}. Both are experimental, i.e they include the reduced mass correction. The hypothetical Rydberg constant R_∞ for an infinite mass nucleus (μ = m) can be calculated from fundamental constants:

$$R_\infty = 10973.731534\ (13)\ cm^{-1} = mc\alpha^2/(2h)$$

where the dimensionless fine-structure constant $\alpha = m_0ce^2/(2h)$ gives the fundamental strength of the electromagnetic interaction

$$\alpha = 7.29735308E\text{-}3\ (33) \approx 1/137\ .$$

The ratio R_H/R_∞ then gives the electron/proton mass ratio, etc.

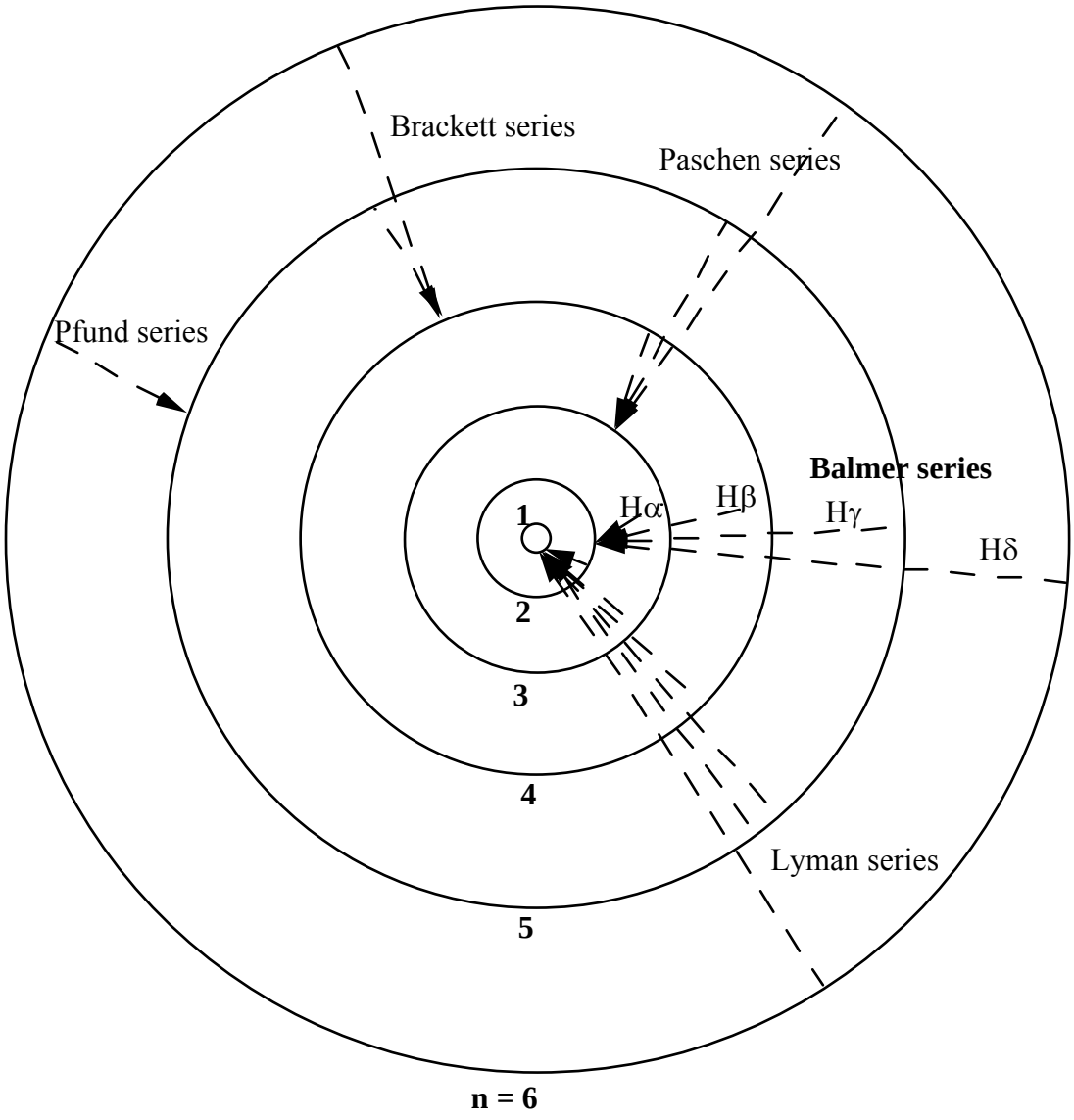

Quantum jumps up to $n_i = 6$, giving rise to the different spectral series

The series are named for early atomic spectroscopists. Radii of circular Bohr orbits are to scale; lengths of arrows are not proportional to photon energies.

Further structure to the Balmer energy levels arises from the intrinsic ("intrinsic spin") angular momentum of an electron. (Electrons are fermions, which have half-integer (in $h/2\pi$ units) intrinsic angular momentum. Bosons have integer intrinsic angular momentum, e.g. the photon which has intrinsic angular momentum one in addition to orbital angular momentum.

Electron intrinsic spin $s = 1/2$ couples to electron integer orbital angular momentum l to form total angular momentum $j = l \pm s = j \pm 1/2$, according to

quantum mechanical rules. Thus a Sommerfeld orbit with n = 3 and l = 2 forms two states with j = 5/2 and j = 3/2 (h/2π units). These are split in energy ("spin-orbit splitting"), but not resolved in our observation of the hydrogen spectrum. Similar splittings are easily resolved in neutral sodium or other alkali spectra, with the larger j level usually lying higher.

A "level" with total angular momentum j can exist in a 2j+1 multiplicity of "space orientations" (2j+1 "states"), for any directional axis. In the absence of an external field (e.g. magnetic) these 2j+1 states are "degenerate" (same) in energy . Since the electron is charged, there is a magnetic moment associated both with its intrinsic spin and with its orbital motion, and a net magnetic moment given by the vector coupling of the two separate contributions; the relation between magnetic moment and angular momentum differs for the two types, however. In the presence of a "weak" external magnetic field there is an interaction energy between net magnetic moment and external field which depends on relative orientation and which splits the energy levels into "Zeeman" levels. (A very strong external magnetic field will "de-couple" the net interaction into separate intrinsic and orbital magnetic moment interactions.) We will not observe magnetic splittings in the absence of a field; however the 2j+1 multiplicity of degenerate levels has an observable effect in the relative intensities of transitions of very similar energy between levels of the same intrinsic internal structure (wave functions).

Finally, the planetary atomic picture of Bohr and Sommerfeld gives way to the wave mechanical picture of a distributed electron "cloud" representing the square of a distributed probability wave function which satisfies a wave equation (Schroedinger in non-relativistic treatment, Dirac in relativistic), with boundary conditions appropriate to bound states (continuity and single-valuedness). (This picture does not imply that an electron has an extended distribution; at present the electron seems experimentally to be a point particle. Calculations, however, must average over the wave function representing its spatial and spin probability distribution. In contrast, a nuclear proton has an extended (bound quark) structure; small hyperfine magnetic interaction energy shifts result for electron orbits which penetrate the nucleus (chiefly l = 0 or "s" orbits)).

The "probability cloud" description does not much modify the energy predictions for a single electron atom, but does so for more complicated atoms; however, even small energy shifts are of crucial importance in testing the validity of a fully relativistic theory which includes the intrinsic quantized electron spin. Still further, as mentioned above, relativistic field-theoretical treatment of observable effects such as the Lamb shift extend the picture from one-body (two bodies with conservation of linear momentum) to many-bodies, in the inclusion of interaction of the electron with self-emitted and absorbed "virtual" photons and e+ - e- pairs.

Electron velocities can approach $v/c \approx .01$ for the n = 1 hydrogen orbit (only l = 0 allowed). Use of the Dirac relativistic expression for total energy of a one-electron system with nuclear charge Z increases the predicted transition energies over those given by the simple non-relativistic Rydberg expression (Eisberg &

Resnick, p286):

Eq. 5 $E_{Dirac,\ hydrogenic} = -RZ^2/n^2 * \{1 + (\alpha^2/n)*[1/(j+1/2) - 3/(4n)]\}$,

the shift from the simple Bohr expression then being

Eq. 6 $-R\alpha^2Z^2/n^3 * [1/(j+1/2) - 3/(4n)]$.

The shift clearly falls off rapidly with increasing n. For our data involving different n values, approximating the difference between initial and final state relativistic shifts by that for the final state (smaller n) only gives a result approximately in the range of fit error for the experimental vacuum Rydberg constant, the theoretical shift being usually toward shorter wavelengths (greater transition energy). (However, the calculated upper state transition shift is greater than the lower for the transition n = 3, l = 0, j = 1/2 --> n = 2, l = 1, j = 1/2), so the anomalous net effect in this case is to reduce the transition energy or wave number from that predicted by the simple Bohr theory. In general, the lower state accounts for about 80 - 100% of the net effect; the magnitudes of the net shifts are in the general range 0.05 - 0.5 cm^{-1}, approximately the error in the Rydberg fit.

In principle, the various theoretical Dirac shifts could be weighted by their theoretical relative intensities to obtain a net shift for the unresolved set of lines to be applied as a data correction. However, while the electric dipole sum rules discussed below for the alkali doublet and triplet multiplets should apply to the "allowed" hydrogen transitions between a particular upper l_u ($j_u = l_u \pm 1/2$) and lower l_l ($jl = l_l \pm 1/2$) states, the relative electric dipole transition intensities of unresolved lines starting on differing l_{upper} states of the same n (e.g., n = 3 with l_{upper} = 2, 1 and 0) are not given by the sum rules, since different l_u states and l_l states) have essentially different radial wavefunctions. Theoretical transition rate weightings could be applied, relying on the theoretical wave functions, but the relative populations of the emitting states would depend on specific excitation conditions, whereas members of a multiplet may usually be assumed to be relatively populated according to their statistical factors 2j+1.

These shifts are not particularly large for the hydrogen Balmer series (Z = 1); for inner electron orbits in high Z atoms involved in characteristic X-ray transitions the relativistic effects become substantial. Still further corrections can be made (retarded potential effects, etc.) A series expansion based on pre-Dirac theory can be found in Ruark and Urey.

From the above Dirac expression hydrogen states with the same n and j , but different l, are unsplit (energy "degenerate"), even though the wave functions are quite different (see Eisberg & Resnick, Fig. 8-11, p 286.) However, Willis Lamb showed in 1947 at the Columbia Radiation Laboratory that the l = 0 and 1 hydrogen states with n = 2 and j = 1/2 are slightly split, i n good agreement with the theory of quantum electrodynamics (QED), the first great field theory of physics. (See Eisberg & Resnick, pp. 287-288.) The splitting is explained as due

to the differing interactions of the electrons in the two different states with energy non-conserving (but $\Delta E \times \Delta t$ uncertainty principle observing) self-emitted and absorbed "virtual" photons and, to a lesser extent, with emitted "virtual" electron-positron pairs. For this and a different experiment in the same lab, also involving atomic beam techniques, Lamb and Polykarp Kusch shared the Nobel prize in physics.

The photon has intrinsic angular momentum 1; transitions between two $J = 0$ states are therefore absolutely forbidden by angular momentum conservation. "Selection rules" representing relative probabilities of other types of transitions are based on the vector character of the electric and magnetic fields and on (squared) quantum-mechanical "overlap" transition probability integrals (Heisenberg "matrix elements") involving initial and final state wave functions. These "selection rules" are usually expressed in terms of "allowed" and "forbidden" transitions, where "forbidden" usually means merely much less probable, i.e much longer lifetime against decay.

The "rules" for "allowed" transitions are: Δn unrestricted (but small Δn decays faster than large), $\Delta l = \pm 1$, $\Delta J = 0$ or ± 1, $\Delta m_l = \pm 1$, $\Delta m_s = 0$ (no spin flip), where l refers to the orbital angular momentum of the valence electron. (Strictly speaking, only the angular momentum J of the whole many-electron system is a valid quantum number; in approximation where most electrons of a many-electron atom pair to zero angular momentum, the net J may be attributed mainly to the j of one or more "valence" electrons.) Violations of the above selection "rules" ("forbidden" transitions) can occur, but much more slowly, except for the absolute prohibition $J = 0 =\not> J = 0$ which follows the vector boson(intrinsic spin 1) character of a photon and the absolute conservation of angular momentum. "Forbidden" transitions will be observed very weakly in the presence of competing "allowed" transitions and will require extended observation periods and careful consideration of confounding background, unless no final states exist permitting "allowed" transitions.

"Allowed" transitions with $\Delta l = \pm 1$ have parity change between initial and final states; they are referred to as electric dipole transitions. (Even or odd parity refers to the presence or absence of a wave function sign change when an odd (one or three) number of spatial coordinates (x,y,z) are reflected - i.e, when the coordinate system is switched from right to left-handed.) The parity of a wave function of orbital angular momentum l is $(-1)^l$.

2a. Optical spectra of many-electron atoms

Many-electron atoms and ions are designated as I, II, III, IV etc., where He I is the neutral (two-electron) atom, He II is singly ionized (one electron, hydrogen-like atom), C VI is hydrogen-like, etc. Hydrogen-like ions with $Z > 1$ would follow the general Rydberg formula for bound state energies, but relativistic corrections would be large in comparison with those for hydrogen, as the electron "orbits" (wave function is concentrated) much closer to the nucleus (much higher

electron velocities than for hydrogen).

With many bound electrons a major departure from the Rydberg picture arises from the possibility of one electron being closer to the nucleus than another, either in the electron cloud picture or in the Sommerfeld picture of "inter-penetrating" elliptical orbits, since the attractive central force from the nucleus is no longer simply proportional to -Ze2/r, and since the various electrons have an additional repulsive Coulomb interaction among one and another. A description of individual electron states serves well for successive approximation with the Fermi quantum statistics of identical electrons preventing two electrons having all the same quantum numbers, resulting in atomic electron "shell structure" ("aufbau (build-up) prinzip").

Outer electron states (valence, least tightly bound) are most easily excited by electron impact in a plasma or in other ways. De-excitation transitions among these produce photon emissions characteristic of the atom or ion in the optical range; excitation and following de-excitation among more tightly bound "inner" electronic states produces X-rays characteristic of the charge Ze of the atomic nucleus (i.e. of the element).

A valence electron in an excited bound state sees, approximately, a central nucleus of charge +Z shielded by (Z-1) negatively charged electrons. The binding is therefore approximately Rydberg, but not exactly, due to some penetration of the inner electron "cloud" by the valence electron, lower l orbits being more penetrating. Therefore states with the same principal quantum number n but with differing l values are separated in energy, in contrast to the hydrogen situation, where there is no core electron "cloud" to penetrate. Excitation of the single valence electron of alkali atoms produces optical spectra resembling that of the hydrogen atom with, however, splitting of the spin-orbit states $j = l \pm 1/2$ into easily observable doublets.

2b. Optical spectra of alkali atoms.

The hydrogen atom is the alkali atom par excellence, but splittings are difficult to observe optically with a grating spectrometer. The optical spectra of neutral alkali atoms, such as atomic sodium (Z = 11, which involves a single valence electron outside a closed shell (spherically symmetric charge distribution) of 10 "inner" electrons) consists of spectral "doublets" and "triplets", referred to generically as "multiplets".

These alkali multiplets (and other, more complicated spectra) give (along with "anomalous" Zeeman splitting in an external magnetic field) an explicit manifestation of intrinsic (electron) fermion spin. Protons and neutrons are also fermions, following their three-fermion (three-quark) internal structure. (Relativistic quantum theory requires all particles obeying fermion statistics to have half-integer intrinsic spin, and all obeying boson statistics to have integer spin. Note that the neutral sodium atom consists of 34 fermions (11 electrons, 11 protons and 12 neutrons), and therefore obeys boson statistics. See the discussion

of boson condensation in rubidium atoms in the New York Times of 7/11/95). This optical data was available to theorists long before the advent of such sensitive techniques as electron spin resonance (ESR). For an interesting historical discussion of the struggle toward a theory of this fundamental intrinsic electron structure see Pais' Physics Today article.

Since there is some penetration of the inner electrons by the alkali valence electron probability "cloud", the state energies are only approximately hydrogenic; however the classification of states by quantum numbers is similar to that for hydrogen. A group of states treated as having the same **L** (vector sum of individual $\mathbf{l}_i$) and **S** (vector sum of individual $\mathbf{s}_i$), with **L** and **S** coupled vectorially to different **J**'s, will normally lie close in energy (split by spin-orbit interaction), and the transitions between two such ensembles is referred to as a spectral "multiplet", with closely lying wavelengths. An alternate coupling scheme, more appropriate to heavier atoms (i.e. a better basis for perturbation calculations), first couples individual electron $\mathbf{l}_i$'s and $\mathbf{s}_i$'s to $\mathbf{j}_i$, then the individual electron j_i are finally coupled to a total state angular momentum **J**. For an alkali atom (e.g., sodium) the states involving excitation only of the single valence electron (l,s,j) have L = l, s = 1/2 and J = j = l ± 1/2, i.e. there is no distinction between the two main coupling schemes.

Recalling that $\Delta l = \pm 1$ with wave function parity change for an allowed electric dipole transition, alkali spectra (one valence electron) include:

Case 1: **<u>Doublets</u>** (two close spectral "lines" where upper or lower state is l = 0 (e.g. upper l = 1 --> j_{upper} = 3/2 or 1/2, with lower l = 0 --> a single j_{lower} = 1/2), or vice-versa[1], and

Case 2: **<u>Triplets</u>** (three close spectral lines, where neither upper nor lower state is l = 0, e.g. l_{upper} = 2 --> j_{upper} = 5/2 or 3/2 with lower l_{lower} = 1 --> j_{lower} = 3/2 or 1/2, ==> 4 possible transitions (2 upper x 2 lower) but with one forbidden (very weak) (e.g. $5/2_{upper}$ --> $1/2_{lower}$), leaving three allowed electric dipole transitions. (In practice, lack of instrumental resolution may sometimes produce the appearance of only two lines).

2b. Relative intensities in multiplet spectra

---

[1] Doublets in the neutral sodium spectrum include: 3p1/2,3/2 --> 3s1/2 (589.0, 589.6 nm) and 7s1/2 --> 3p1/2,3/2 (474.8, 475.2 nm); 6s1/2 --> 3p1/2,3/2 (514.9, 515.3 nm); 5s1/2 --> 3p1/2.3/2 (615.4, 616.1 nm), 4s1/2 --> 3p1/2,3/2 (1138.1, 1140.4 nm). The first will exhibit intensity ratio variability as the vapor lamp heats up, due to increasing absorption from the ground state in increasingly dense "cool" outer vapor where excited states are poorly populated. Correspondingly the other transitions, which do not end at the ground state, should not be absorbed and the intensity ratio should remain more nearly constant as the lamp heats up.

Relative intensities of multiplet members are of great interest because they test basic theoretical expectations concerning the atomic wavefunctions and the transition probability: That the radial part of the wavefunctions should be essentially the same, separately, for the initial and the final states involved in a spectral multiplet and that (because the transition energies of "multiplet" members differ relatively little) the transition probability "phase space factors" (related to kinetic energy release) are also essentially identical. Thus the electric dipole (allowed transition) radial integral squares, and also the phase space factors, closely cancel in the intensity ratios leaving involved in the ratio only "easily" calculated vector photon (spin-one) overlap integrals with initial and final angular wavefunctions, and initial and final statistical state population factors.

(For a single valence electron "outside" of closed "inner electron" shells the spherical symmetry of the attractive potential felt in the initial and final states by the valence electron leads to separation of the valence-electron initial and final wavefunctions into products of radial, polar angle and azimuthal angle parts (in the appropriate spherical coordinate system). Therefore the transition rate-governing square of the initial and final state "operator overlap integrals" also simplifies into three separately treatable pieces each depending on only one of the coordinates (r, θ, ϕ) (in spherical coordinates).

In 1924, before the advent of wave mechanics and the Schroedinger equation, Burger and Dorgelo proposed a "sum rule" for "narrow"

multiplets:

> "The sum of the intensities of all lines of a (spectral) multiplet which come from a given initial level is proportional to the quantum weight of that level; and the sum of the intensities of all lines of a multiplet which end on a given final level is proportional to the weight of that level" (Ruark & Urey, p699; see also footnote on p 698).

Here quantum weight = $2j+1$ (the number of "Zeeman" or spatial orientation states, energy degenerate in the absence of a magnetic field).

A wave mechanical discussion for spherically symmetric wavefunctions is given by Sobelman, pp. 211-214, who concludes, in agreement with Burger & Dorgelo:

> "Therefore, when
>
> $$N1:N2 = (2j_1+1):(2j_2+1)$$
>
> (this occurs, for example, with a Boltzmann distribution[2] with temperature

[2] However, in the common case of an electrical discharge light source (Herzberg, pp 159-160) "where excitation results from collisions with electrons of all possible velocities, the Boltzmann factor plays no very significant part. Or, expressing this in another way, the temperature of the electron gas is so high that $e^{-E/kT}$ can be taken equal to 1 for most of the states in question." In both cases (i.e., thermal excitation or

> kT >> $\Delta E(j_1,J_2)$, it is possible to formulate the following rule for the relative intensities of the multiplet components:
>
> The sum of the intensities of all lines of a multiplet, having one and the same initial level, is proportional to the statistical weight of the given level. A similar rule also holds for all lines of a multiplet having one and the same final level."

These "sum rules" indicate that, for the strongest sodium (yellow "D" lines) doublet (case 1 above) where there is only one final (lower) j_l (n = 3, l = 0, j = 1/2) and two initial (upper) levels (n = 3, l = 1, j_u = 1/2 or 3/2), and where the spectral lines are easily resolvable, we should expect the 3/2 --> 1/2 (5890 Angstrom Units (1 Å = 10 nanometers) observed transition strength (count rate) to be twice that of the 1/2 --> 1/2 (5896 Å) transition, and Ruark and Urey cite an experimental ratio of 100:49 (p701).

> [In fact, the first quantitative local measurement with the Spex 1 meter grating spectrometer gave too low a a ratio, about 1.23 instead of the initial state statistical factor of 4:2 = 2. For the similar doublet pair with only one final j_2 (n = 3, l = 0, j_l = 1/2) and two initial (upper) states (n = 4, l = 1, j_u = 1/2 or 3/2) the ratio was 1.26. (Here, however, the separation of the observed peaks was much less than for the strong, yellow doublet.)
>
> Spectrometer efficiency could not vary much over these small wavelength intervals. The (unlikely) possibility of severe differential rate-dependent losses in the photomultiplier or in the computer data processing software was eliminated by observing the "D" lines ratio while varying the intensity from a hot sodium discharge with crossed polaroids. Further investigation showed that the expected 2:1 ratio is obtained in the first four minutes or so of warmup of a cold Na vapor discharge; thereafter the ratio decreases with increasing vapor temperature and corresponding pressure). A plausible explanation involves a hot central vapor discharge region where the initial intensity ratio is 2:1 (5890/5896) and a cooler outer vapor region where the Na vapor atoms are mainly in their ground states and can absorb and re-emit in all directions, thus removing photons incident on the spectrometer. This occurs differentially according to the 2:1 ratio of statistical factors for the two upper (now final) states: $\sigma(5890) = 2\sigma(5896)$ (omitting small λ^2 factors). (See Sobelman). As the photons pass through a length w of the cooler absorbing vapor region, the relative number of photons changes as
>
> $$I(5890)/I(5896) = (\text{initial intensity ratio}) \times \exp\{-\sigma(5890)w\}/$$

---

elecric discharge excitation) the relative populations of states with nearly equal energies is $N_n/N_m = g_n/g_m$. For non-equal energies, with electric discharge excitation, the Boltzmann factors will be nearly equal, in contrast to the situation for thermal equilibrium excitation.

$$\exp\{-\sigma(5896)w\}$$

$$= 2\exp\{[\sigma(5890)-\sigma(5896)]w\} = 2\exp\{\sigma(5890)w\}$$

$$(\ \sigma(5890) = 2x\sigma(5896)\ ).$$

The final observed ratio from a hot discharge is an accident of the particular lamp configuration, equilibrium temperature, etc.

In contrast, for the resolved doublet with a single initial (upper) state (n=7, l = 0, j_u = 1/2) and two final (lower) states (n=3, l=1, j_l = 1/2 or 3/2) the same experiment gave a ratio of 2.168, in fair agreement with the final state statistical factor ratio of 4:2. Here, even if absorption cross sections are significant, there are few excited states populated in the "cool" outer vapor regions and absorption cannot occur readily. Thus these photons from the interior hot region of the discharge escape unscathed.

Application of the dipole sum rules to Case 2 ("diffuse" spectral triplet (an apparent "doublet") + unobserved fourth "forbidden" transition) is illustrated in matrix form by White[3], p120 :

		2p 3/2	2p 1/2
		4	2
2d 5/2	6	**X**	**0**
2d 3/2	4	**Y**	**Z**

where the integer numbers are the statistical 2j+1 factors and intensity 0 has been entered for the forbidden (magnetic quadrupole) transition. Then, taking ratios to eliminate a common constant of proportionality, we have from the sum rules:

$$X/(Y+Z) = 6/4 \text{ and } X+Y/Z = 4/2,$$

two equations in three unknown intensities. However we do not seek the absolute quantities, but only the relative intensities in smallest whole number ratios. Then the equations are satisfied by

$$X = 9,\ Y = 1 \text{ and } Z = 5.$$

If the two d terms are close so that the corresponding spectral lines are unresolved (our case), the total intensity of the d transitions is 10 and the ratio of the (apparent) doublet intensities is 10:5. For four such cases (upper d (l=2) states

[3] See Herzberg, p 161, for a similar treatment of the ^2P - ^2D transitions.

with n = 9, 8, 7, 6 and common lower p (l=1) states (n=3)) reported ratios are respectively 2.434, 2.030, 1.861, and 2.171, with a mean of 2.124.

Thus agreement with theory is fair except for the strongly emitted true doublets, where absorption of emerging photons in cool, outer vapor is also strong.

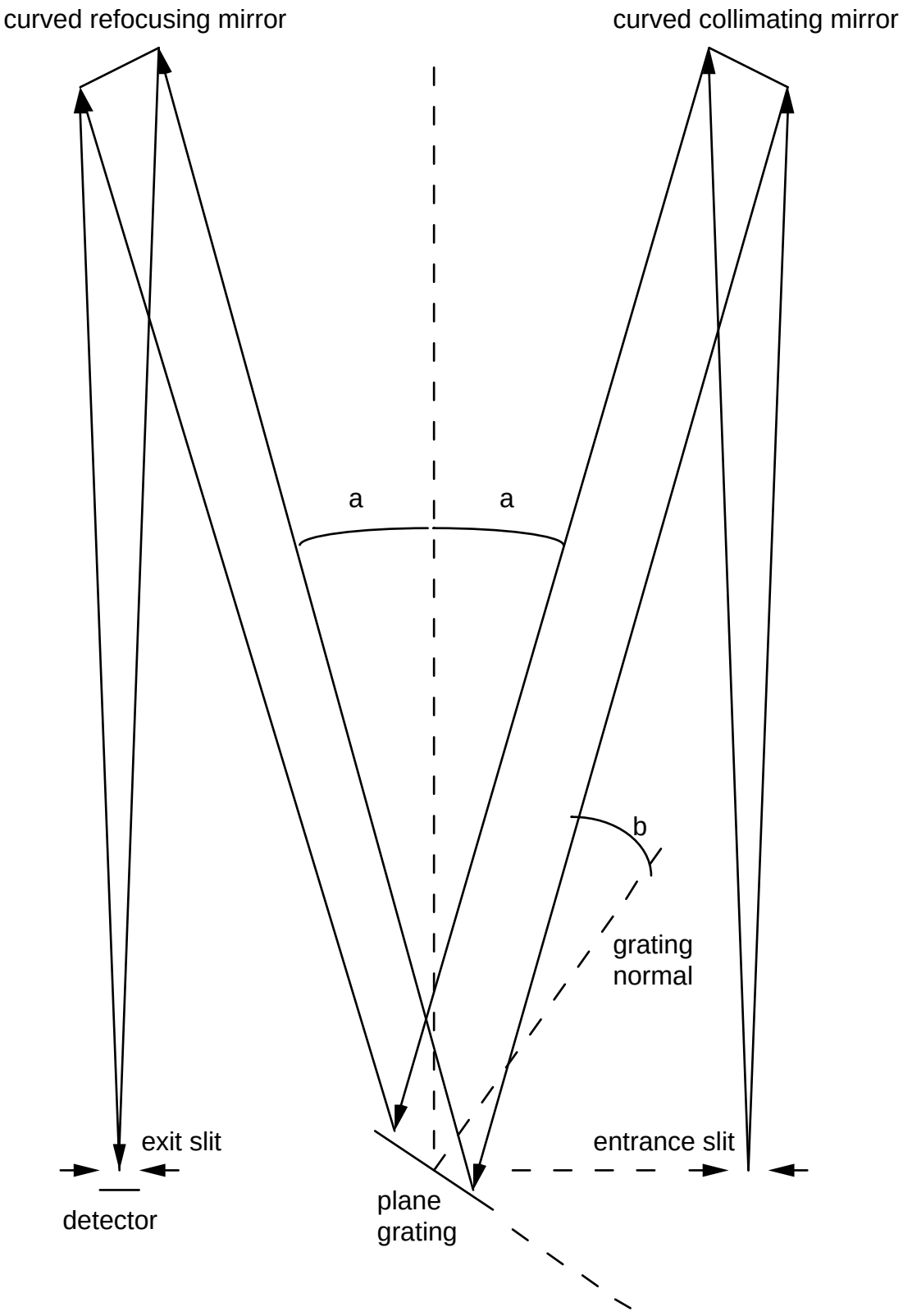

Czerny-Turner scanning optical grating spectrometer

II Apparatus

1. Grating Spectrograph

In a simple grating with plane wave normally incident, the entire transmission spectrum available between $\theta = 0$ and $\theta = \pm 90$ degrees can be viewed by rotating the observing telescope about the grating center. In principle one could place a detector array or film strip in the focal plane and detect all wavelengths at once. For this case

Eq. 7 $$n\lambda = d\sin(\theta).$$

In contrast, for the Czerny-Turner scanning spectrometer, the direction of incidence and the direction of observation are both fixed. A limited angular range of incident rays of all wavelengths passes the entrance slit and strikes the first (collimating) mirror which renders them parallel and directs them toward the grating. Constructive interference from the overlapping diffraction patterns of individual grooves then directs rays from a narrow range of wavelengths to strike the second mirror and be refocused through the exit slit onto the detector. Other constructive interference patterns miss the second mirror and are not observed (except for possible scattering within the system). One can detect only an ext limited range of wavelengths at once.

The physical path difference (the optical path difference is modified by the index of refraction of air) between rays striking adjacent grating "grooves" with spacing d has contributions from the incident and exit rays

Eq. 8 $$d\sin(b) + d\sin(2a+b) = 2\sin[1/2(2a+2b)]\cos[1/2(b-(2a+b)]$$

$$= 2\cos(a)\sin(a+b)$$

where a is the fixed angle formed by either mirror center and the grating center and b is the variable angle between grating normal and rays incident on the grating. The condition for observation of an interference maximum with the Czerny-Turner geometry is then

Eq. 9 $$ml = 2\cos(a)\sin(a+b)\ .$$

Rotation of the grating varies b and thus the observed wavelength. Resolution is determined by the system size, grating quality and the width of the adjustable entrance and exit slits. The grating does not rotate as far as $b = -a$ (grating normal parallel to the system center line), which would represent the mirror reflection angle ($m = 0$) at which all wavelengths are refocused toward the exit slit.

Grating grooves can be formed by "ruling" (gouging parallel grooves with a precision "ruling engine" or by holographic pattern formation by subsequent etching or by ion bombardment. The Spex 1000M holographic grating has 1800 lines per millimeter. Holographic gratings are free of "ghosts", false spectral lines

due to periodic imperfections in ruling engine screws. The effective area of the large grating is reduced with an "aposidising" ("without feet") diamond shaped mask, which increases the line width (reduces resolution) and also reduces the intensity by about 4x but, as a trade-off, reduces the nearby small secondary maxima (the "feet"of the strong transition) by about 1000x, thus improving greatly the ability to detect weak transitions of wavelength close to that of a strong transition. (For discussion of line shape and aposidising masks see James.)

The 1995 Edmund Scientific Annual Reference Catalog, p69, has this to say about holographic gratings (the type employed in the Spex 1000M):

> "Holographic gratings are formed by an interference fringe field of two laser beams, whose standing wave pattern is exposed to a polished substrate coated with a photo resist. Processing of the exposed medium results in a pattern of straight lines with a sinusoidal cross section. Holographic gratings produce less stray light than ruled gratings. They can also be produced with up to 3600 grooves per millimeter for greater theoretical resolving power. Due to their sinusoidal cross section, holographic gratings cannot be easily blazed and their efficiency is usually considerably less than a comparable ruled grating. There are, however, special cases which should be noted. When groove spacing to wavelength ratio is near one, a holographic grating has virtually the same efficiency as the ruled version. A holographic grating with 1800 grooves per millimeter has the same efficiency at 500 nm as a blazed ruled grating. Holographic master gratings are replicated by a process identical to that used for ruled gratings."

The Spex spectrometer, as for many reflecting devices using incidence near the grating normal, fails in the ultraviolet due to increasingly poor reflectivity; grazing incidence instruments are then used, usually with vacuum light paths to minimize air absorption. For wavelength-efficiency curves, including 1800 lines/mm, see the '95 Edmund catalog, p69.

Factors affecting the shape of spectral lines include a) natural line width (inverse to decay lifetime (according to the Heisenberg uncertainty principle), b) Doppler (temperature) broadening ($\Delta\lambda/\lambda = 7.16 \times 10^{-7}$ sqrt(T/m)), c) instrumental line shape and d) pressure broadening (collisional lifetime shortening). Effects a) and b) produce Gaussian line shapes; c) produces sinc^2 and sinc^4 shapes, with and without apodising [$\text{sinc}(\theta) = \sin(\theta)/\theta$]. The natural width will not be observable with the Spex spectrometer. For a discussion of these shapes and their net result, and of apodising masks, see James.

The plot below shows wavelength vs. angle b for 1800/mm and a = 30 degrees. Angle b is taken as + to the right, - to the left of the incident rays as seen from the grating. The near linearity between wavelength and angle is due to the approximate validity of the small angle approximation for $|b| < 30$ degrees.

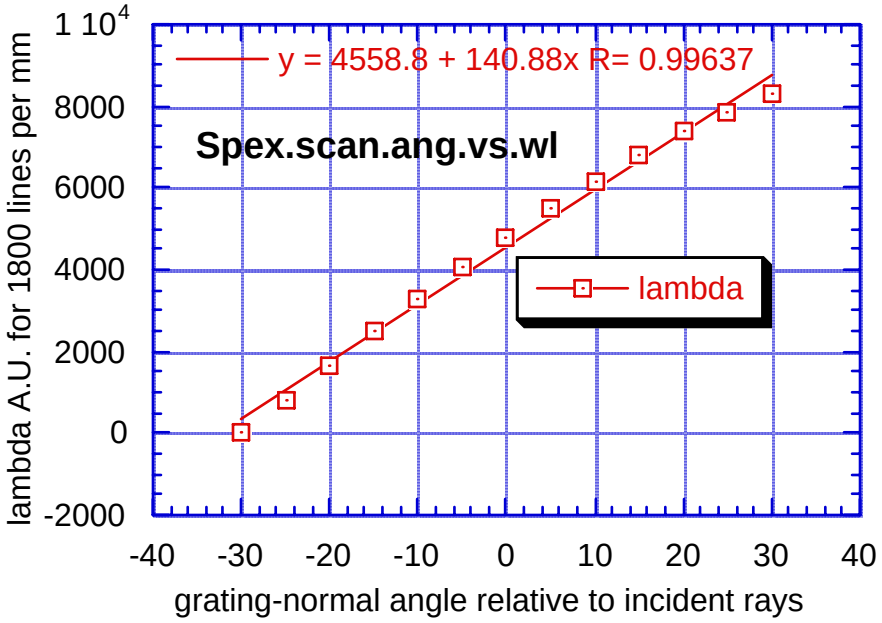

A "sine bar" riding at right angles to a precision drive screw makes sliding contact with a pin attached to a grating mount crank arm, producing exact linearity (within screw accuracy) between linear motion of the bar and sin(a+b) and thus a linear relation between screw rotation and wavelength. Interpolation is provided by counting pulses to the stepping motor drive of the screw. A mechanical counter outside the spectrometer box indicates wavelength. For a grating of 1200/mm, the ratio is 1, for wavelength in Angstrom units (1 Å = 10 nm); for the 1800/mm grating, the counter reading is 1.5 x wavelength (Å).

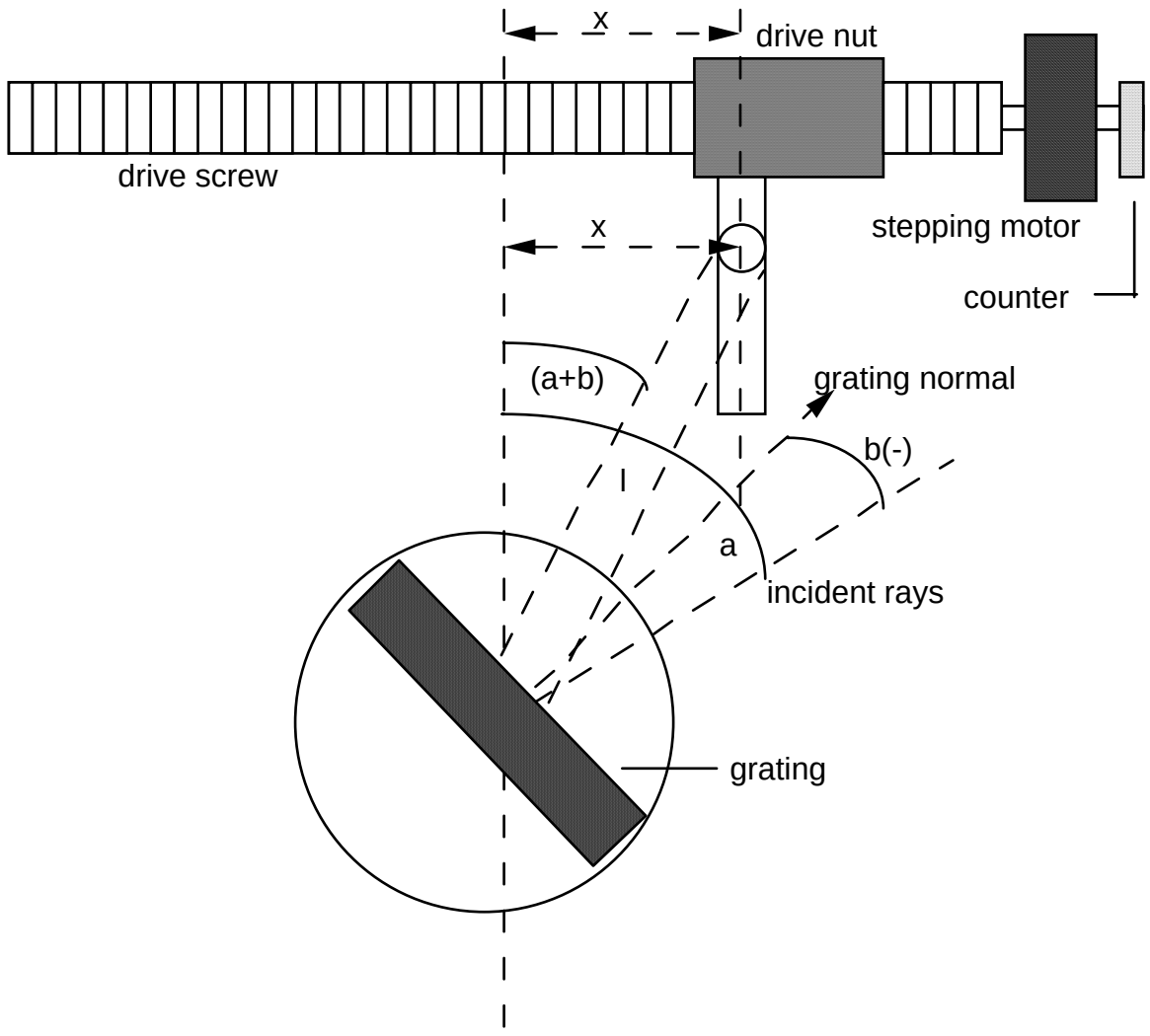

Conceptual sine bar drive. Angle b is negative, according to previous convention.

Eq. 10 $x/l = \sin(a+b) = \{ m/[2*\cos(a)] \} * \lambda \quad (m = 1)$

Side entrance and exit slits are provided for a second source and detector. Mirrors swing into place to divert the entrance rays toward the collimating mirror and/or the exit rays toward a side-window photomultiplier photon detector. The direct exit rays impinge without exit slit on a photon diode array (PDA) of 1024 counters, each 25 microns wide by 2 mm high, allowing a range of wavelengths to be observed simultaneously, thus increasing efficiency of data taking. However the phototube has much lower background and is more suitable for precision or for low light intensities. It has also greater quantum efficiency at shorter wavelengths than the PDA. We will not use the PDA for this experiment.

For both types of detector charge is collected to provide an analog signal, then read out via an analog to digital converter (ADC) and stored in a 16 bit word, the conversion calibrated in quantized charge-releases (counts). However, counting rate is usually

indicated graphically. The 16 bit word size limits the maximum counting rate which will be indicated for a spectral peak to 2^{16}/accumulation time; e.g., for an accumulation time of 0.1 seconds, higher real rates will result in an apparent peak rate closely equal to $2^{16}/0.1 = 655{,}360$ counts per second, etc. The indication that counts are being lost due to the word size limitation is a "flat-topped" peak appearance.

The entire apparatus is computer controlled. Data analysis options are available for determining peak areas, channel counts/second, peak wave lengths (per prior calibration) etc. Re-calibration is normally not needed, if the grating is reset to the 5000 Å position before shut-down.

III Data acquisition

1. Familiarization

Using a mercury discharge spectrum, set the spectrometer for known strong spectral lines. Scan at different wavelength step sizes using the phototube. Practice recording peak wavelengths and peak areas (counts per second x Å calculated by acquisition program from counts and accumulation time - not counts) and background levels. Note and record any strong non-mercury lines observed from this source. Some strong lines are: 2536.5 Angstrom units (g), 3125.67 - 3131.55 - 3131.84, 4358.3, 5460.7 Å ("g" denotes that the lower transition level is the ground state; the line is referred to as a "resonance" line.) The quartz glass permits ultraviolet lines to pass. This uv lamp should be turned on only when it is mounted on the entrance slit of the spectrometer. This will prevent looking at the uv light which can hurt the eyes.

The prominent mercury spectral lines involve excitation of electrons from the ground state configuration consisting of two 6s electrons $(6s)^2$ plus an inert core of 78 electrons. Note from an energy-level, transition diagram (e.g., Grotrian diagrams by Stoner and Bashkin on the reserve shelf of the Physics library,) and in the brief Zeeman discussion below, that allowed (electric dipole) transitions do not involve relative electron spin-flip (intercombination lines); e.g. triplet states (two parallel electron spins) decay to triplet states and singlet states (two anti-parallel electron spins) decay to singlet states. Intercombination transitions can occur, but are typically slow, and therefore weak.

When setting wavelengths, observe carefully whether the units are to be specified as nanometers (nm) or as Angstrom (Å) units.

Using the Spectramax software observe the lines at 5460.7 and 4358.3 Å should be easily visible with an integration time of 0.1 second (try and see). The line at 3125.7 Å may be invisible at 0.1 second, but clear at 10 seconds; you may not be able to see the very strong line at 2536.5, even at 100 seconds, due to the source tube-glass ultraviolet cutoff and decreasing grating reflectivity.

You should be able to see the 3125.7 line at 0.01 second integration time. However, you may still be unable to see the 2536.5 Å "resonance" (ground state)

line. The Handbook of Physics and Chemistry gives the following relative UV line intensities:

Wavelength (Å)	Relative Intensity
3131.84	320
3131.55	320
3125.67	400
2536.52	15,000

See the Edmund Scientific '95 catalog, p69, for typical variation of grating efficiency.

The spectrometer calibration is usually set using a strong known mercury line, e.g., 4358.3 Å.

(This 4358.3 Å line (6s7s $^3S_1$ --> 6s6p $^3P_1$ transition), and that at 5460.7 Å (6s7s $^3S_1$ --> 6s6p $^3P_2$), exhibit the "anomalous" Zeeman energy splitting , proportional to the strength of an external magnetic field. The current laboratory Zeeman magnet produces about 1 tesla at 8 amperes. You will see the Zeeman effect easily at 0.5 tesla because of the spectrometers excellent resolution and sensitivity.

A mercury line of interest for observation of the "normal" Zeeman effect in an external magnetic field lies at 4046.6 Å. ("Normal" means that the Zeeman spectrum consists of only three equally spaced lines, as predicted by Zeeman for classical electron orbits in a magnetic field; the nomenclature is historic and archaic. For the 4046.6 line (6s7s $^3S_1$ --> 6s6p $^3P_0$ atomic states) only three magnetic levels are observed in the external field, with M_z = +1, 0, -1. "Anomalous" Zeeman spectra exhibit more lines, corresponding to the quantized and coupled orbital and spin angular momenta and their associated magnetic moments. From a quantum mechanical point of view, the "anomalous" spectra are the rule, and the "normal" are the exceptions.)

2. Alkali doublets in sodium

You will take 4 spectra of the sodium D doublets, 5890 - 5896, as the lamp heats up. You will observe how the relative peaks of the two lines change. Set Trace Mode to Overlayed. Do not touch the mouse during scanning. Take 4 spectra sequentially that demonstrate the change in the relative peaks of the two lines. When this run is complete be sure it is saved; allow the lamp to cool down and

repeat for another sodium doublet which does not involve the ground state[1]. Analyze the two multispectra runs for peak areas. (Check for flat-topping.) Enter beginning clock time or run number and peak areas into Kaleidagraph; calculate the area ratio for each doublet and plot the ratios vs. clock time or run number.

Use the Grotrian diagram for Na I (neutral sodium, NaII = singly ionized, etc.) of Bashkin and Stoner (Physics Library reference shelves) to suggest possibly observable multiplets and their wavelengths. Record peak wavelengths, peak areas, and phototube background; in your report, give area ratios within multiplets and compare with theory. For the very strong yellow doublet reduce either the accumulation time (≤ 0.1 seconds will probably be necessary) or the intensity (using crossed polaroids) until neither peak is flat-topped (peak counts $< 2^{16}$ --> peak rate $< 2^{16}$/accumulation time).

You will probably find the peak area ratios (units counts per second x Angstrom units) for the strong true doublets (5890 & 5896, 3302.37 & 3302.98 Å) to be considerably less than the theoretically expected 2:1 (3/2:1/2 upper or lower states, respectively).

3. Balmer transitions in hydrogen

Here accurate determination of wavelengths is paramount, for comparison with theory. Calculate the expected wavelengths for the first 5 or 6 Balmer transitions in hydrogen. What accuracy do you attribute to the wavelengths? What precision? (Use known Hg lines as calibration. According to grating theory, an absolute determination of wavelength would follow determination of the grating line spacing and of the diffraction angle.)

Scan these lines at high resolution (e.g. 0.05 Å step size or less) using phototube detection. (Turn off the hydrogen tube when not needed for data acquisition; it warms up quickly.) Select dwell time to obtain good statistics. For longer wavelengths, a second or less per step may do; at shorter wavelengths, 5 seconds per step might be needed.) Record peak wavelengths (interpolating, if needed) and areas (note linearity limit from sodium observations). Save spectra against possible future need.

The best system resolution obtainable with narrow slits is about 0.005 Å

TURN OFF THE HYDROGEN LAMP WHEN NOT SCANNING

4. Balmer transitions in deuterium

Repeat the above, using a deuterium discharge tube. This will also show hydrogen lines. Record the deuterium wavelengths for various n and (as well as possible) the H - D wavelength differences.

TURN OFF THE DEUTERIUM LAMP WHEN NOT SCANNING

IV Data analysis

1. Sodium doublets

Make a table showing paired observed doublet or (unresolved) triplet accepted and experimental wavelengths, transition assignments for the observed lines (i.e., n,j,l values (s is always 1/2) for initial and final states, experimental peak areas, area ratios between observed multiplet members (probably several transitions with $j_{upper} = 5/2$ and 3/2 ($l_{upper} = 2$) will be unresolved), and the theoretical intensity ratios (add in case of unresolved lines for the case where an actual triplet appears as a doublet, due to lack of resolution). Maintain the order, i.e., if shorter wavelength (higher transition energy) is given first, then give all other corresponding quantities first.

2. Balmer series and Rydberg constants

Data acquisition is wavelength in air, Rydberg theory in energy (inverse wavelength or wavenumber).

For both hydrogen and deuterium make tables of observed transition wavelengths, labeled by initial and final state n, l and j values. (Spin-orbit splitting will not be observed, i.e. there will be more theoretical transitions than observed, due to limited resolution. Group all unresolved theoretical resolutions.)

Correct hydrogen and deuterium observed wavelengths to vacuum values using the wavelength-dependent index of refraction of air and include in the table. (The effect is to increase the wavelength ($v_{vacuum} = c > v_{air}$, $f_{vacuum} = f_{air}$). Interpolate between entries of the air-index tables in the handbook of Chemistry and Physics.) Enter also in the table the accepted tabular vacuum wavelengths, and check for any apparent systematic (calibration offset) discrepancy between experimental and tabular vacuum wavelengths. (The data fit to theory will allow for such a common term.)

Invert and enter in the table the corrected experimental vacuum wavelengths to obtain corresponding wave numbers (inverse length units, proportional to transition energy).

(Ignore the Dirac relativistic correction (see Eisberg and Resnick, p 286)

$$\Delta T(n,j) = R\alpha^2(Z/n)^4\,[n/(j+1/2) - 3/4] \approx 5.82*Z^4/n^3\,[n/(j+1/2)-3/4]\ cm^{-1}$$

where α is the fine structure constant $e^2/(\text{hbar } c) \approx 1/137$.

The difference between relativistic shifts could be calculated between the final ($n_f = 2$, $j = 1/2$) states and upper (n_i) states involved in the transition; the net effect is to increase the experimental wavenumber (proportional to transition energy) above that given by the simple Balmer formula. If unresolved transitions are present in the observed peak, each relativistic correction ought to be weighted by

relative occurrence and an average shift calculated. However, because of the $1/n^4$ factor, the shift in the lower state will dominate.)

Plot corrected wave number data against $(1/n_f^2 - 1/n_i^2)$ ($n_f = 2$). (Use KaleidaGraph or other program.) Estimate a typical wavenumber uncertainty from estimated wavelength experimental uncertainties and perform a two parameter, non-linear weighted least square fit. (In KG select relevant rows and scatter-plot first (no fit without plot), then:

Curve Fit --> General, Fit1, Define: **m1+m2*m0; m1=?;m2=?**.

m0 = the independent parameter ("x"), m1 through m9 are adjustable fitting parameters. Reasonable initial search values must be assigned; never use zero.) Assign estimated wavelength errors, uniform or otherwise as you judge. In KG this will constitute a separate weight column. For a weighted fit the reduced chi square total for the best fit is meaningful. For an unweighted fit, KG assigns an arbitrary, uniform weight of one to all data points, and the chi square is not meaningful.)

Save this plot and fit and include in your report with fit equation, fit parameter errors and reduced chi-square value.

Compare the m1 fit parameter with its error. If the m1 uncertainty is ≤ the m1 value, try a refit without m1. Report both results. This term could represent a systematic calibration error. The net relativistic correction might be ≈ .2 Å Correcting the data for the offset term m1 and performing a new linear fit should not affect the Rydberg determination, so there appears to be no point to further analysis.

Calculate the discrepancies between your experimental Rydberg values (slopes m2) and the accepted values for hydrogen and deuterium. Scale discrepancies to your final errors in your Rydberg parameter, m2.

From the ratios of R_H and R_D to R_∞ determine the experimental reduced mass corrections, and thence the ratios of electron to proton and to deuteron masses. Give the errors in these ratios.

Since we assume all the physical constants in $R\infty$ to be well known, including the electron mass, the proton and deuteron masses and the ratio m_d/m_p can be calculated from the two values of $m/m_{nucleus}$. Include these calculated values.

In fair approximation the ratio md/mp can be directly calculated from $(R_D-R_0)/R_H-R_0)$, where averaging has occurred in the best fit determination of R_D and R_H), or by averaging for the various values of n the ratios $(\Delta\lambda_H/\Delta\lambda_D)_n = (\lambda_H-\lambda_0)_n/(\lambda_D-\lambda_0)_n$. This is due to the smallness of the electron mass, relative to the nuclear masses involved, as can be easily seen:

$\Delta R_H/\Delta R_D = (R_0-R_H)/(R_0-R_D) = R0(1-\mu H/m)/R0(1-\mu D/m)$

$= \{[(1-m_p/(m+m_p)]/[(1-m_d/(m+m_d)]\} = \{[m/(m+m_p)]/[m/(m+m_d)]\}$

$= (m+m_d)/(m+m_p)$.

Dividing numerator and denominator by m_p

$\Delta R_H/\Delta R_D = (m_d/m_p+m/m_p)/(1+m/m_p)$

where all terms are small except $(m_d/m_{p)}$ and 1. One can drop the two small terms (leaving $\Delta R_H/\Delta R_D = m_d/m_p$, or substitute from the value of R_H the derived value of m/m_p.

The ratios $(\Delta\lambda_H/\Delta\lambda_D)_n$ give the same expressions for m_d/m_p. An average, or weighted average over n, can be used.

Calculate m_d/m_p using these two ratio methods.

Appendix 1 Spectrometer operation

STARTUP PROCEDURE:

On the shelf below the spectrometer are the computers that run the SPEX system. To the far left is a UPS (Uninterruptable Power Supply) that is always left on. This conditions the line voltage and gives you a 2 minute window to shutdown things if there is a power failure (it has a battery in it). It should be "on" at all times.

To the right of the UPS is the SPEX MSD 2 (stepper motor controller) box. It should normally be "on". If not, call Dr. Mike Molnar (Room 202) for help.

To the right of the SPEX MSD 2 is the Spectraco computer. This, too, should be always left "on". If not, turn it on and WAIT. One of the two red lights will come on the SPEX MSD 2. (The upper light indicates setting for PDA accumulation; lower , for PMT scan.) This computer will beep and start reading the bootable floppy (green light on floppy drive.) When the Spectraco computer is done reading, it will beep a second time: now you can proceed to the next step.

To the right of the Spectraco is a second computer, a DELL PC. **TURN IT ON**. Push the center button. If the monitor is not "on", turn it on too.

A menu pops up. Hit "enter" to accept the first (1) mode: Spectramax for Windows.

OPTION #2 gives you the old software (worthless offal); OPTION #3 is DOS.

Hit the spacebar after the memory check.

Once in Windows select Spectramax and select YES for all questions.

A new window opens: Instrument Control Center. Select the first button: Run Experiment. Again, say YES to any questions.

A new window pops open. Familiarize yourself with it.

Go under **COLLECT** and select **Experiment**. There are a number of "canned" experiments that you can select. This will set the wavelengths and integration times automatically.

Alternatively, you can change the starting and ending spectral positions to what you need. The start must be less than the end. MAKE SURE THESE ARE CORRECT. - A mistake can make you lose calibration of the instrument. Example: you want a line at 4861Å. So, start at 4850.0Å and end at 4870.0Å and use 0.1Å steps at the default integration time (might be 0.01 s).

Select **RUN**. DO NOT TOUCH ANYTHING (KEYBOARD OR MOUSE) WHILE THE SPECTROMETER IS SCANNING.

Under **FILE** select **PRINT**.

Make copies for both lab partners.

QUIT:

Do not save anything.

Exit Spectramax.

Exit Windows.

Turn off ONLY the DELL PC and PRINTER.

DO NOT TURN OFF THE SPECTRACO OR UPS!!